Oxydehydrogenation of propane over Mg–V–Sb-oxide catalysts. II. Reaction kinetics and mechanism

James N. Michaels, David L. Stern and Robert K. Grasselli [1]

Mobil Technology Company, Strategic Research Center, PO Box 1025, Princeton, NJ 08543, USA

Received 9 February 1996; accepted 9 September 1996

Recently we reported that $Mg_4V_2Sb_2O_x$ is selective for propane and *n*-butane oxydehydrogenation at low hydrocarbon conversion, and that propane is oxidized in parallel reactions to propylene and CO_x. We report now on the kinetics of propane and propylene oxidations over this catalyst. The partial oxidations of propane and propylene and zero-order in oxygen, whereas deep oxidations of both hydrocarbons are half-order. This difference in reaction order indicates that different forms of reactive oxygen are involved in the partial and deep oxidation reactions. Presumably, nucleophilic lattice oxygen partakes in the partial oxidation, while electrophilic dissociatively adsorbed oxygen is involved in deep oxidation. A single activated surface adsorbed state of the hydrocarbons is thought to be involved in both the partial and deep oxidation reactions. An interpretation of the observed reaction kinetics in context of the $Mg_4V_2Sb_2O_x$ solid state chemistry, and the partial oxidation literature in general, suggests that selective oxydehydrogenation of propane occurs on isolated (Sb–O–V–O–Sb) sites, deep oxidation on multiple vicinal vanadium sites (Sb–O–V–O–V–O–Sb), and partial oxidation of propylene to acrolein on subsurface V-promoted antimony sites (Sb–O–Sb). Therefore, improved selectivity of desired intermediates (propylene/acrolein) should be achieved by further lowering the vanadium concentration and/or through key solid state positioning of the vanadium in the catalyst lattice. Alternatively, selective doping to electronically decrease the electrophilicity of the waste forming sites and its appended oxygen should also help depress the waste forming reaction channels in favor of the desired partial oxidation channels. Finally it is anticipated that higher useful product yields would be attained with a compositionally optimized Mg–V–Sb-oxide catalyst by opting for a more stable, isolatable intermediate, e.g., acrylonitrile, by reacting propane in the presence of ammonia and oxygen (air) over this catalyst.

Keywords: oxydehydrogenation; propane; propylene; Mg–V–Sb-oxide catalyst; reaction kinetics; mechanism; site isolation

1. Introduction

Oxidative upgrading of light paraffins to the corresponding olefins, diolefins, and/or oxygenated products is a topic of current commercial interest [1,2]. Recently, the composition $Mg_4V_2Sb_2O_x$ was identified as a potentially promising light paraffin oxydehydrogenation catalyst [3], and its propane oxydehydrogenation reaction network has been worked out [2].

In these earlier studies [3], it was shown that the useful product selectivity of the base composition $Mg_2V_2O_x$ [4,5] is greatly improved by doping the base with elements such as Sb, Sb–P, or B; with $Mg_4V_2Sb_2O_x$ emerging as one of the more promising compositions for further study. An analysis of the reaction network of propane oxidation [2] reveals that propylene is the only first formed desired product, and that CO_x is produced both by sequential oxidation (through propylene) and by direct deep oxidation of propane. The presence of two parallel pathways to CO_x is of interest, as it suggests that partial and deep oxidation may occur at different surface sites or involve distinct forms of reactive oxygen. If this hypothesis is correct, it may be possible by modification of the catalyst to eliminate the deep oxidation sites or the electrophilic oxygen associated with these sites by proprecious doping or active site isolation, thereby improving the partial oxidation selectivity of this catalyst.

An investigation of the reaction kinetics of propane oxidation may provide insights into these mechanistic issues. Oxidation reactions on reducible metal oxide catalysts occur by two different generic mechanisms: intrafacial, by reaction with lattice oxygen from the catalyst; or suprafacial, by reaction with adsorbed oxygen on the catalyst surface [6]. These two mechanisms are often distinguished by the dependence of the oxidation rate on oxygen partial pressure: intrafacial reactions are commonly zero-order in oxygen, while suprafacial reactions are typically half- or first-order in oxygen (particularly at high temperature and low oxygen partial pressures).

In order to shed some additional light onto the catalytic behavior of $Mg_4V_2Sb_2O_x$, and how it might ultimately be improved through compositional or operational manipulations to achieve enhanced yields of desired intermediate products, e.g., propylene, the current study, dealing with the kinetics and the reaction mechanism of propane oxidation over this system, was undertaken.

---

[1] To whom correspondence should be addressed. Present address: Department of Chemical Engineering, University of Delaware, Newark, DE 19716-3119, USA and Department of Physical Chemistry, University of Munich, Sophienstrasse 11, D-80333 Munich, Germany.

2. Experimental

The synthesis and characterization of $Mg_4V_2Sb_2O_x$, as well as reaction conditions and analytical methodology for their catalytic evaluation have been described previously [2,3].

The reaction kinetics reported here were measured in the temperature range 400 to 550°C and 1 atm total pressure using a conventional fixed bed reactor [2,3].

3. Results and discussion

3.1. Reaction orders

3.1.1. Propane oxidation

Propylene, CO and CO_2 were the only products detected in propane oxidation over $Mg_4V_2Sb_2O_x$. The rates of production of these species, measured between 450 and 500°C at constant propane concentration of 26 mol%, are plotted against the oxygen mole fraction in fig. 1. The partial oxidation rate (rate to propylene) is zero-order in oxygen above 10 mol% oxygen. This behavior is common for partial oxidation reactions on metal oxide redox catalysts [7]. In such catalytic systems, a hydrocarbon is oxidized by reaction with nucleophilic lattice oxygen, and the resulting oxygen lattice vacancy is replenished, directly or indirectly, by subsequent reaction with gaseous oxygen. If the rate of replenishment of lattice oxygen is rapid compared to the rate of removal, the concentration of the lattice oxygen at the catalyst surface is independent of the prevailing oxygen partial pressure, and the rate of hydrocarbon oxidation is zero-order in oxygen. This behavior is exhibited in the current study by the rate of propylene production, suggesting that partial oxidation of propane over $Mg_4V_2Sb_2O_x$ is an intrafacial reaction between propane and lattice oxygen of the catalyst.

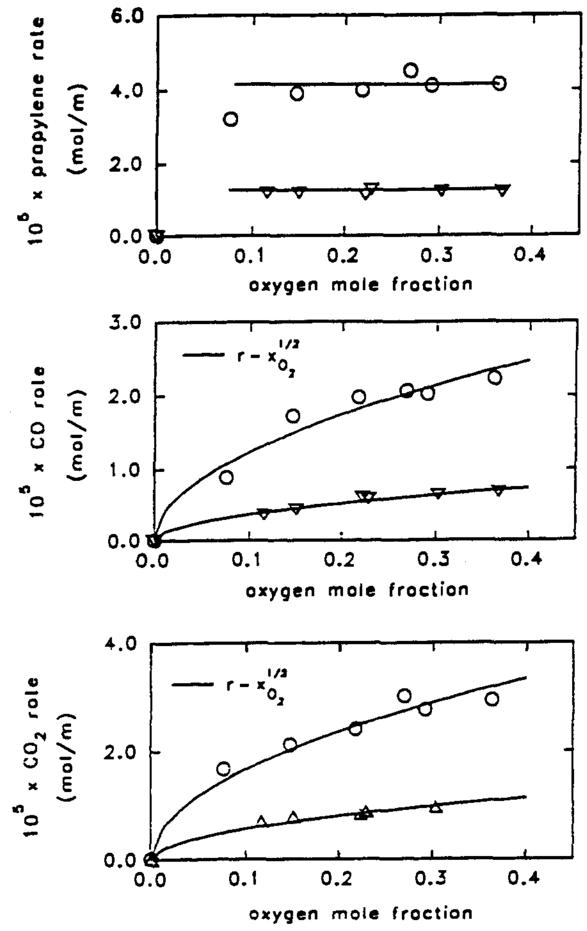

Fig. 1. Propane oxidation kinetics over $Mg_4Sb_2V_2O_x$: oxygen concentration dependence. Feed propane mole fraction: 0.26. (▽) 450°C; (○) 500°C.

In contrast, the rates of deep oxidation of propane to both CO and CO_2 increase monotonically with oxygen concentration. This indicates that deep oxidation of propane occurs by reaction with a distinct form of oxygen, different from that involved in partial oxidation. As shown in fig. 1, the data can be fitted by rate expressions half-order in oxygen. Half-order reactions are common in heterogeneous catalytic systems in which one of the reactants in the rate-determining step is dissociatively adsorbed. The data suggest that deep oxidation of propane on $Mg_4V_2Sb_2O_x$ is a suprafacial reaction between propane and dissociatively adsorbed oxygen.

The rates of propylene, CO, and CO_2 production measured between 470 and 530°C at 30% oxygen concentration are illustrated in fig. 2. The rates of all three reactions are less than first-order in propane. As discussed in greater detail below, the data can be fitted with a "Langmuir-type" rate expression:

$$r \propto \frac{kx}{1+Kx}, \tag{1}$$

in which x is the propane mole fraction, and k and K are constants. This type of rate behavior is common in heterogeneous catalytic systems and typically indicates that the rate-determining step of a reaction involves a species that is in adsorption equilibrium with the gas phase. In this case, k is a rate constant and K is an adsorption equilibrium constant.

3.1.2. Propylene oxidation

Acrolein, CO, and CO_2 were the only products detected in the oxidation of propylene over $Mg_4V_2Sb_2O_x$. The rates of production of these species were measured as functions of oxygen and propane mole fractions between 400 and 490°C, with the data indicating that the kinetics of partial and deep oxidation of propylene are quite similar to those of propane oxidation over this catalyst.

As shown in fig. 3, the rate of partial oxidation of propylene to acrolein is zero-order in oxygen, at least at oxygen concentrations in excess of 10 mol%. Conversely, the rates of CO and CO_2, are well described by a rate expres-

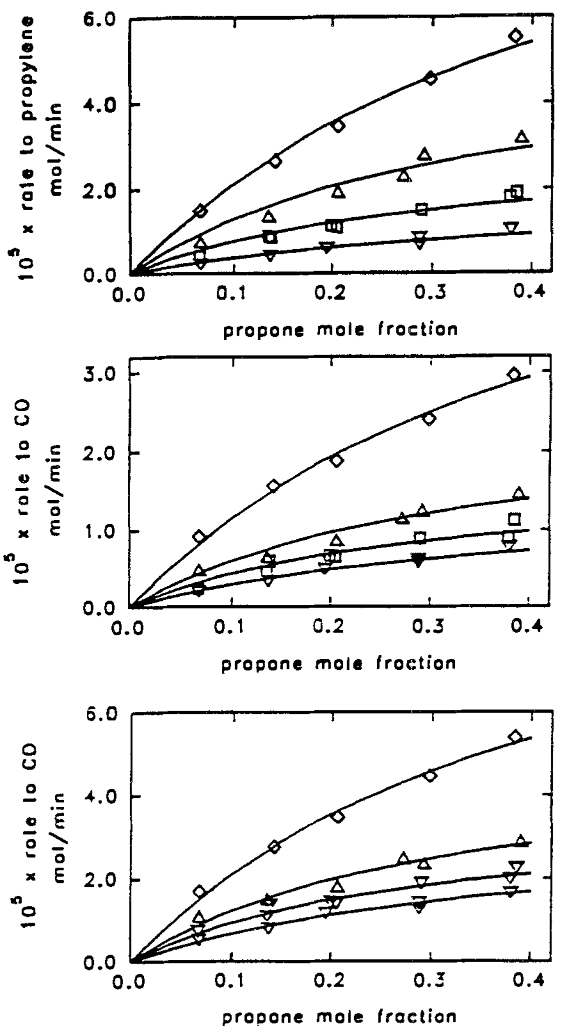

Fig. 2. Propane oxidation kinetics over $Mg_4Sb_2V_2O_x$: propane concentration dependence. Feed oxygen mole fraction: 0.30. (◇) 530°C, (△) 500°C, (□) 475°C; (▽) 450°C, (—) calc.

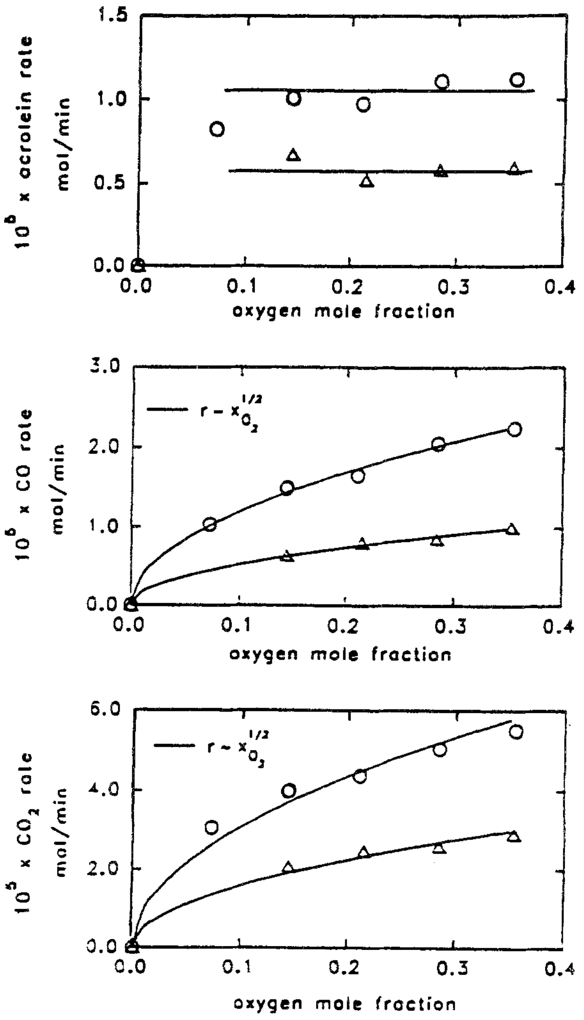

Fig. 3. Propylene oxidation kinetics over $Mg_4Sb_2V_2O_x$: oxygen concentration dependence. Propane mole fraction: 0.20. (△) 440°C, (○) 445°C.

sion that is half-order in oxygen. Therefore, as in the case of propane, partial and deep oxidation of propylene involve different forms of reactive oxygen, or different catalytic sites. The kinetics of acrolein production suggest that partial oxidation occurs by reaction of propylene with lattice oxygen. The kinetics of CO_x production suggest that deep oxidation occurs by reaction of propylene with dissociatively adsorbed oxygen.

The partial and deep oxidation rates are all positive-order in propylene (fig. 4). The data fit well a Langmuir-type rate expression, suggesting that propylene is in adsorption equilibrium in all reactions. At low temperatures and high propylene concentrations, the reaction rates approach constant values; indicative in Langmuir–Hinshelwood kinetics that the catalyst surface is saturated with the hydrocarbon. Importantly, there is no tendency for the rates to become negative-order in propylene at high concentrations. Such behavior, if observed would be indicative of propylene and oxygen adsorbing competitively [8]. Therefore, the data suggest that propylene and oxygen adsorb on distinct sites on the catalyst surface of $Mg_4V_2Sb_2O_x$.

3.2. Kinetic model

The kinetics of propane and propylene oxidation over $Mg_4V_2Sb_2O_x$ suggest that partial and deep oxidations of the two hydrocarbons occur by two distinctly different mechanisms. The two mechanisms differ primarily in the form of reactive oxygen involved in the rate-determining step. Partial oxidation of propane can be described by a Mars–Van Krevelen mechanism in which adsorbed hydrocarbon reacts with lattice oxygen:

$$C_3H_8 + \sigma_{HC} \rightleftharpoons C_3H_8(a) \qquad \text{fast, reversible} \qquad (2)$$

$$C_3H_8(a) + O_O \rightarrow C_3H_6 + V_O \qquad \text{rate-determining} \qquad (3)$$

$$O_2 + 2V_O \rightarrow 2O_O \qquad \text{fast} \qquad (4)$$

in which (a) denotes an adsorbed species, σ_{HC} is a hydrocarbon adsorption site, and O_O and V_O are a lattice

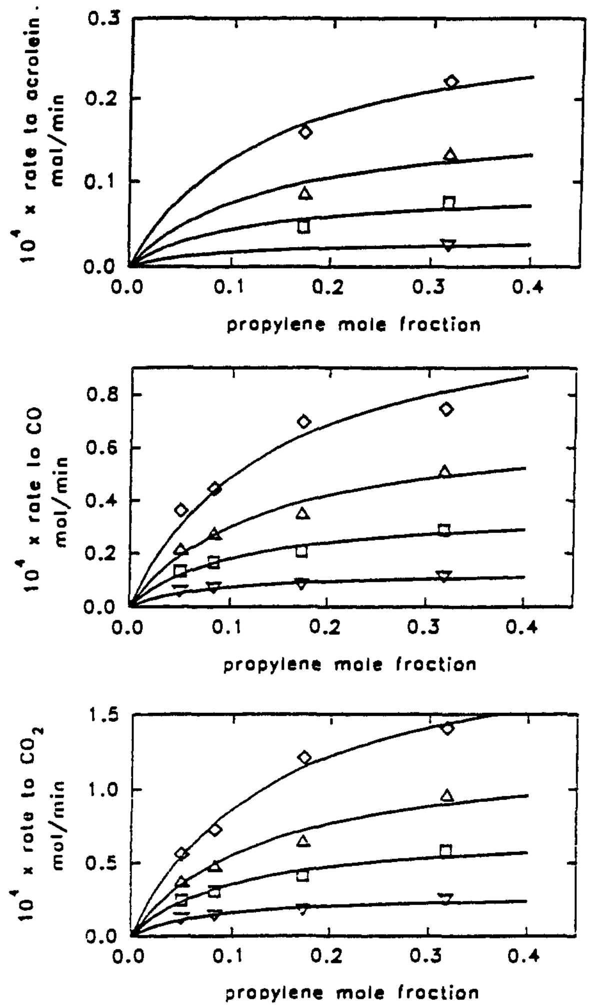

Fig. 4. Propylene oxidation kinetics over $Mg_4Sb_2V_2O_x$: propylene concentration dependence. Feed oxygen mole fraction: 0.30. (◇) 490°C, (△) 465°C; (□) 440°C, (▽) 400°C, (—) calc.

oxygen and lattice oxygen vacancy, respectively. In contrast, deep oxidation of propane can be described by a Langmuir–Hinshelwood mechanism in which adsorbed hydrocarbon reacts with dissociatively adsorbed oxygen:

$$C_3H_8 + \sigma_{HC} \rightleftharpoons C_3H_8(a) \quad \text{fast, reversible} \qquad (5)$$

$$O_2 + 2\sigma_O \rightleftharpoons 2O(a) \quad \text{fast, reversible} \qquad (6)$$

$$C_3H_8(a) + O(a) \rightarrow CO_x \quad \text{rate-determining} \qquad (7)$$

in which σ_O is an oxygen adsorption site. Since oxygen and the hydrocarbons adsorb on different surface sites, their adsorption is non-competitive. Propylene oxidation can be described by an analogous set of reactions in which propylene replaces propane in reactions (2) and (3), and acrolein replaces propylene in reaction (3). Simple rate expressions can be derived from these two mechanisms under the following assumptions: First, the rate-determining steps are assumed to be first-order in each reactant. Second, propane, propylene, and oxygen are assumed to be in adsorption equilibrium, and their surface coverages are described by the Langmuir isotherm; the oxygen coverage is assumed to be small. Third, reoxidation of the catalyst surface, described by reaction (4), is rapid enough that the surface remains fully oxidized during reaction; in this case, the concentration of lattice oxygen is constant and is independent of the prevailing gas-phase composition and temperature. Finally, under the reaction conditions of this study, the concentrations of all products in the gas phase were small, therefore, their surface coverages are assumed to be negligible. Rate expressions for partial and deep oxidation of propane are derived in the appendix. Under these constraints, the partial oxidation rate of propane to propylene is described by:

$$r_{Pr} = \frac{k_{Pr}x_{C_3}}{1 + K_{C_3}x_{C_3}} \qquad (8)$$

and the deep oxidation rates of propane to CO and CO_2 are described by:

$$r_{CO} = \frac{k_{CO}x_{C_3}x_{O_2}^{1/2}}{1 + K_{C_3}x_{C_3}}, \qquad (9)$$

$$r_{CO_2} = \frac{k_{CO_2}x_{C_3}x_{O_2}^{1/2}}{1 + K_{C_3}x_{C_3}}. \qquad (10)$$

In these expressions, x_{C_3} and x_{O_2} are the mole fractions of hydrocarbon (propane or propylene) and oxygen in the gas phase, respectively, k_{Pr}, k_{CO}, and k_{CO_2} are rate constants of propylene, CO, and CO_2 production, and K_{C_3} is the propane adsorption equilibrium constant. It is important to note that these rate expressions share a common adsorption equilibrium constant; this follows from the model assumption that a single adsorbed state of propane takes part in all three oxidation reactions. Oxidation of propylene to acrolein, CO, and CO_2 is described by an analogous set of rate expressions in which x_{C_3} and K_{C_3} refer to propylene rather than propane.

The rate expressions are consistent with the experimental observation that partial oxidation of propane and propylene are zero-order in oxygen and deep oxidation of the two hydrocarbons are half-order in oxygen. They also have the Langmuir-type dependence on the hydrocarbon mole fraction, described by eq. (1). The expressions were fitted to the propane oxidation rate data in fig. 2 using a single adsorption equilibrium constant at each temperature, and the calculated rates are shown by the solid curves. The good agreement between measured and calculated rates indicates that the kinetic model is consistent with the data over the entire range of gas compositions and reaction temperatures investigated. Similar agreement is found between the model and the propylene oxidation rate data (fig. 4).

Rate and adsorption constants were determined from the least-squares fit of the model rate expressions to the data (table 1, figs. 5 and 6). Within the scatter of the data, the rate constants vary exponentially with inverse tem-

Table 1
Kinetic model parameters: rate and adsorption constants in propane and propylene oxidation over $Mg_4V_2Sb_2O_x$

Propane oxidation

	Temperature (°C)			
	450	474	500	530
$10^4 \times k_{Pr}$ (mol/min)	0.47 (±0.2)	1.04 (±0.04)	1.72 (±0.07)	2.63 (±0.05)
$10^4 \times k_{CO}$ (mol/min)	0.68 (±0.2)	1.09 (±0.04)	1.47 (±0.05)	2.61 (±0.05)
$10^4 \times k_{CO_2}$ (mol/min)	1.57 (±0.2)	2.34 (±0.05)	3.00 (±0.06)	4.78 (±0.07)
K_{C_3}	2.58 (±0.90)	3.55 (±1.00)	3.27 (±0.5)	2.37 (±0.56)

Propylene oxidation

	Temperature (°C)			
	400	440	465	490
$10^4 \times k_{Ac}$ (mol/min)	0.40	0.89 (±0.12)	1.34 (±0.14)	2.21 (±0.11)
$10^3 \times k_{CO}$ (mol/min)	0.29 (±0.15)	0.63 (±0.08)	0.94 (±0.10)	1.47 (±0.07)
$10^3 \times k_{CO_2}$ (mol/min)	0.63 (±0.34)	1.23 (±0.06)	1.72 (±0.08)	2.60 (±0.32)
K_{C_3}	12.9 (±4.8)	9.84 (±3.4)	7.77 (±3.1)	7.22 (±1.5)

perature, and the activation energies of all reactions lie between 16 and 25 kcal/mol (table 2, figs. 5 and 6).

The adsorption equilibrium constants should also vary exponentially with inverse temperature according to:

$$K_{ads} = e^{\Delta S_{ads}/R}\, e^{-\Delta H_{ads}/RT}, \qquad (11)$$

in which ΔS_{ads} and ΔH_{ads} are the entropy and enthalpy of adsorption. The propylene adsorption constant, shown in fig. 6, obeys eq. (11) well with an enthalpy of −6.9 (±0.7) kcal/mol and an entropy of −5.1 (±0.9) e.u. These values are indicative of a relatively weakly bound but immobile chemisorbed state of propylene. The pro-

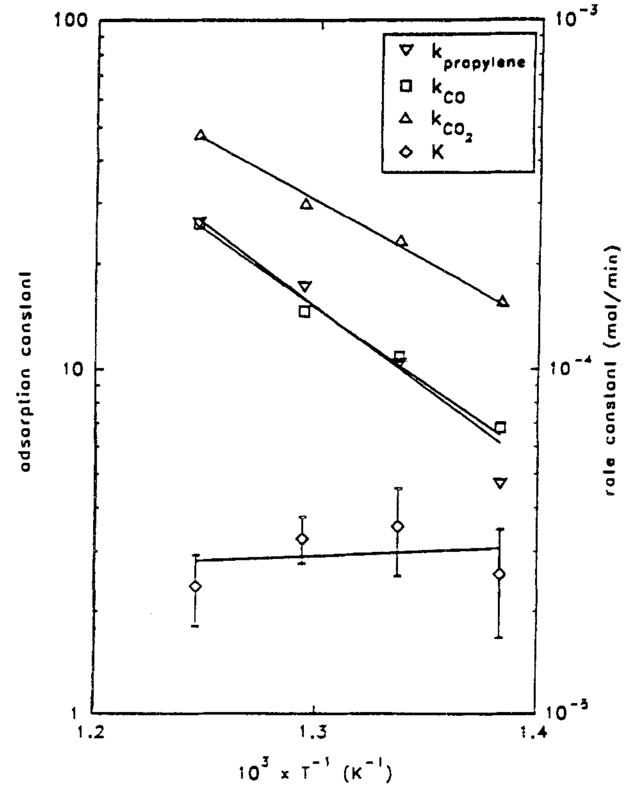

Fig. 5. Rate and adsorption constants of propane oxidation over $Mg_4Sb_2V_2O_x$.

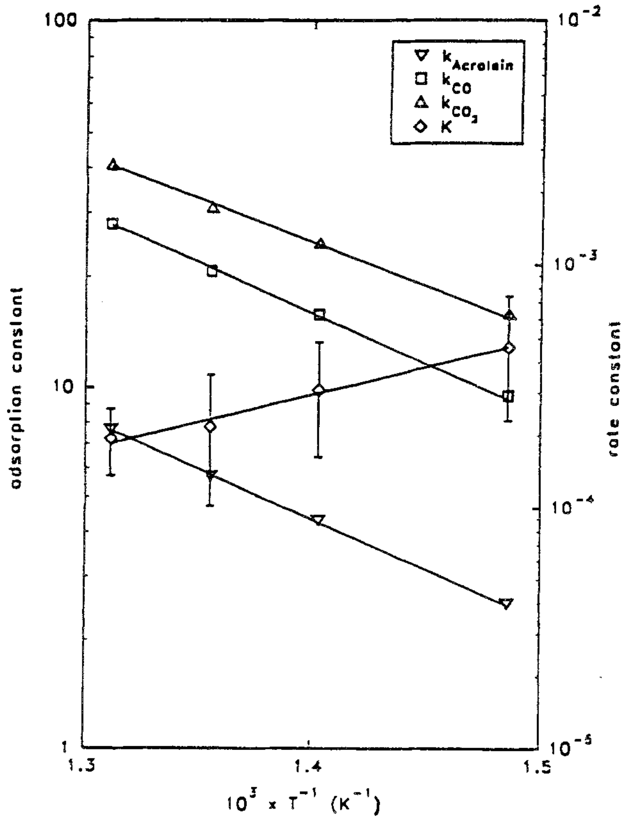

Fig. 6. Rate and adsorption constants of propylene oxidation over $Mg_4Sb_2V_2O_x$.

Table 2
Activation energies and adsorption enthalpies

	Propane	Propylene
activation energy (kcal/mol)		
partial oxidation	24.7 (±2.7)	18.8 (±0.3)
deep oxidation to CO	18.9 (±1.3)	18.2 (±0.4)
deep oxidation to CO_2	15.6 (±0.5)	15.9 (±0.5)
heat of adsorption (kcal/mol)	−1.5 (±4.4)	−6.9 (±0.6)
enthalpy of adsorption (e.u.)	0.1 (±5.8)	−5.1 (±0.9)

pane adsorption constant is less well-behaved. However, as shown in fig. 5, eq. (11) fits these data within their uncertainty; the enthalpy and entropy determined from this least-squares fit are −1.5 (±4.4) kcal/mol and 0.1 (±5.8) e.u, respectively. Given the large uncertainty of these values, it is risky to draw conclusions about the state of chemisorbed propane. However, the very low heat of adsorption may indicate that propane adsorbs dissociatively, forming an adsorbed propyl radical as the reactive species on the surface. Whatever its structure, it is clear from the magnitude of the adsorption constants that the surface coverage of propane is less than that of propylene over the range of conditions studied, indicating that the heat of adsorption of propane is significantly less than that of propylene.

3.3. Mechanistic implications

In our initial study of the Mg–V–Sb-oxide system [2], we suggested that the addition of certain metals to the percent magnesium vanadate system might improve the oxidative dehydrogenation selectivity of the base by modifying the oxidation state and electronic structure of the active vanadium centers, and possibly modify its selectivity behavior through structural site isolation. We showed that addition of antimony produced a significant improvement in useful product selectivity over the base composition, and that the improvement might be due to the formation of a ternary $Mg_{1-x}SbV_{2/3x}O_{3.5}$ phase, the stabilization of a lower vanadium oxidation state, and the interaction with a supra-surface Sb-oxide phase. A slightly different explanation for the improvement was thought to lie in the observed formation of $VSb_{1-x}O_{4-1.5x}$ and its intimate interaction with the $Mg_2V_2O_x$ and supra-surface antimony oxide phases [2]. In either of the two possible explanations, structural site isolation [13] plays an important role. We draw now on these results, those of the reaction network study [3], the kinetic study reported here, and oxidation catalysis literature in general, to speculate about the nature of the catalytic sites involved in partial and deep oxidation of propane on $Mg_4V_2Sb_2O_x$. Through such an analysis we might be able to identify the underlying reasons for the still somewhat disappointing selectivity behavior of this catalyst and gain insights into ways to improve it.

As is well known, vanadium is a common component in oxide catalysts effective for paraffin activation. It forms readily an inorganic radical (V–O· or V^{4+}=O) capable of activating paraffins through hydrogen abstraction, including the activation of such inert molecules as methane [9]. It is hypothesized that in the activation of propane the V–O· radical is responsible for abstracting at least the first (methylene) hydrogen from propane in its conversion to propylene. As noted above, the low heat of adsorption of propane may indicate dissociative adsorption, with the first hydrogen abstraction possibly occurring in concert with propane adsorption. Once adsorbed, a second hydrogen can be abstracted from the adsorbed propyl radical, producing propylene which subsequently desorbs. The second hydrogen is likely abstracted by lattice oxygen; if this step is rate-limiting, the rate of propylene production would be zero-order in oxygen, as observed. In analogy to a mechanism proposed for partial oxidation of propylene to acrolein on antimony-containing ammoxidation catalysts [10], we assume that the lattice oxygen responsible for the second hydrogen abstraction is associated with antimony in $Mg_4V_2Sb_2O_x$. These anticipated reaction steps form the basis of the mechanism of propane oxidation to propylene as shown in scheme 1, where the active site is an isolated vanadium ion surrounded by antimony ions.

Partial oxidation of propylene to acrolein may occur by a similar mechanism. However, vanadium is not a necessary component of the active site for olefin oxidation, and antimony alone can abstract hydrogen from, and insert oxygen into, propylene. Such a mechanism has been proposed for propylene oxidation to acrolein on antimonate catalysts [10] and is summarized in scheme 2. In this mechanism, a hydrogen is abstracted

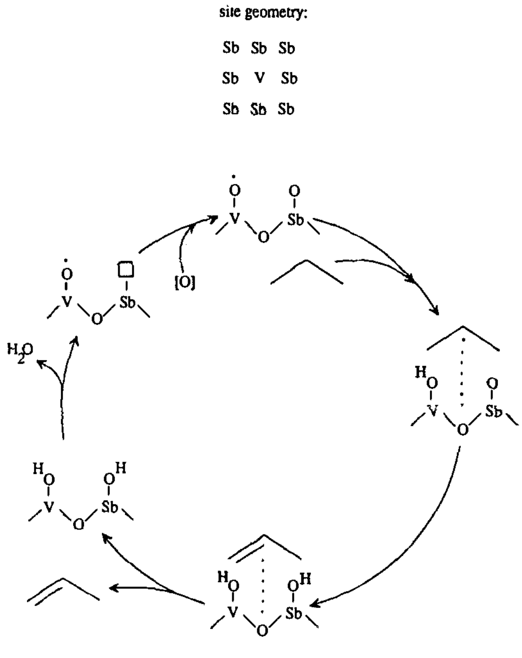

Scheme 1. Mechanism of propane oxidation to propylene.

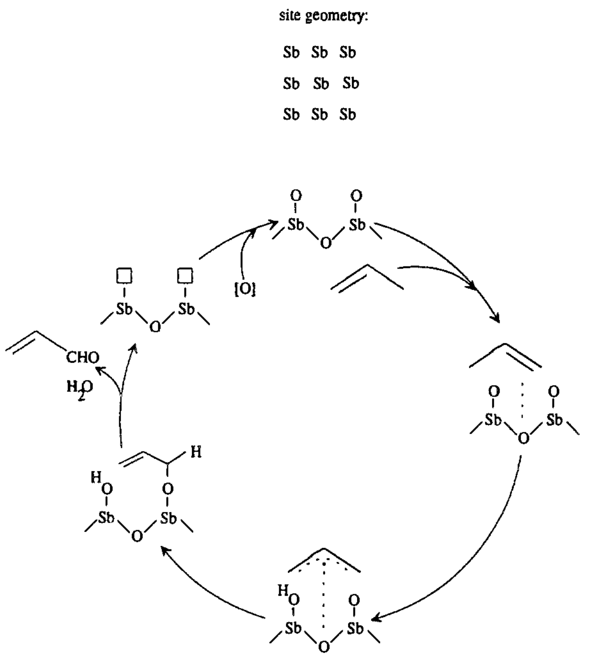

Scheme 2. Mechanism of propylene oxidation to acrolein.

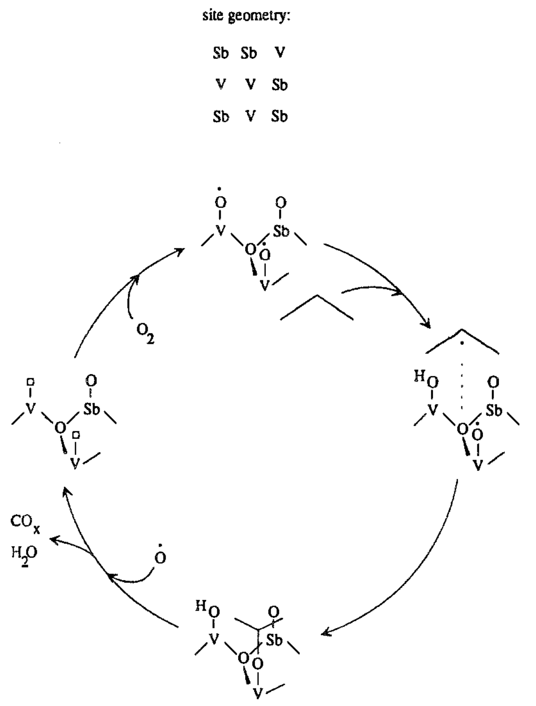

Scheme 3. Mechanism of propane oxidation to CO_x.

from adsorbed propylene by a lattice oxygen to form a π-allyl radical. An adjacent lattice oxygen is inserted into the radical in the rate-limiting step, and acrolein and water desorb. The two remaining oxygen lattice vacancies are subsequently oxidized to regenerate the active site. It should be noted that a V–O· moiety is also able to abstract a hydrogen from adsorbed propylene. Therefore, the mechanism of scheme 2 could also occur on the same site proposed for propane oxidation. However, most likely with lower selectivity, because an exposed vanadium site would easily overoxidize the adsorbed acrolein product to waste products before it could successfully desorb from the surface. It should be emphasized that while Sb-only sites (subsurface promoted by design through redox elements such as V, Fe, U, Ce, etc.) can activate and oxidize olefins, they are totally benign and inactive towards paraffins.

A common feature in schemes 1 and 2 is that nucleophilic lattice oxygen reacts with an adsorbed hydrocarbon radical to produce either propylene or acrolein. In contrast to the mild oxidizing character of nucleophilic oxygen, electrophilic oxygen is known to oxidize organic species to CO_x [11]. Thus, if propane or propylene adsorbs on an antimony center with multiple vicinal vanadium ions, it is likely that the hydrocarbon will be overoxidized to CO_x by the electrophilic oxygen associated with the vanadium ions. This is the basis of the deep oxidation mechanism for propane proposed in scheme 3. As discussed earlier, the reaction kinetics indicate that a common adsorbed state of propane takes part in partial and deep oxidation reactions. Thus, in the first step of the mechanism, a hydrogen atom is extracted by V–O· to produce the same adsorbed propyl radical produced in scheme 1. This radical reacts with a vicinal V–O· to form an unstable alkoxy species [12] that subsequently reacts with additional electrophilic oxygen to produce CO_x and water. Finally, oxygen adsorbs dissociatively on the free vanadium centers to restore the active site. Propylene would be oxidized to CO_x by an analogous mechanism in which either chemisorbed propylene or the π-allyl radical would react with vicinal V–O·.

We can use these proposed reaction mechanisms as a working hypothesis for suggesting ways to modify $Mg_4V_2Sb_2O_x$ and improve its partial oxidation selectivity. Following the well established site isolation theory [13], we can reason that the critical difference between the proposed partial and deep oxidation mechanisms (schemes 1–3) is the local density of vanadium ions around the hydrocarbon adsorption site. Sites selective for partial oxidation of propane and propylene contain no more than one vicinal vanadium ion (Sb–O–V–O–Sb). Sites with more than one vanadium ion promote deep oxidation (Sb–O–V–O–V–O–Sb). This suggests that $Mg_4V_2Sb_2O_x$ is too rich in vanadium. Because we do not know at this juncture the exact extent to which magnesium, antimony and vanadium form a solid solution (there are indications for its presence in Mg–V–Sb-oxides [2]), our arguments will be limited to an interaction between antimony and vanadium, whose solid solution $VSb_{1-x}O_{4-1.5x}$ [14] was definitely observed in the $Mg_4V_2Sb_2O_x$ system [2]. Since the V : Sb ratio in this catalyst is unity, and if the vanadium and antimony ions were to mix homogeneously, their distribution on the surface can be represented by scheme 4a. All of the antia

V Sb V Sb V
Sb V Sb V Sb
V Sb V Sb V
Sb V Sb V Sb
V Sb V Sb V

$VSbO_5$

b

V Sb Sb V Sb
Sb Sb V Sb Sb
V Sb Sb V Sb
Sb Sb V Sb Sb
V Sb Sb V Sb

$VSb_2O_{7.5}$

c

V Sb V Sb V
Sb Sb Sb Sb Sb
V Sb V Sb V
Sb Sb Sb Sb Sb
V Sb V Sb V

VSb_3O_{10}

Scheme 4. Vanadium and antimony ion distribution in VSb_yO_x ($y = 1, 2, 3$).

mony ions are associated with more than one vanadium ion, and this is consistent with the poor partial oxidation selectivity of this catalyst. Reducing the V : Sb ratio by a factor of 2 (scheme 4b) still results in the existence of contiguous vanadium chains, and certain antimony sites having as many as three vanadium neighbors. Only when the V : Sb ratio is cut to 1/3 (scheme 4c) are the vanadium ions suitably dispersed to yield a selective catalyst, they are structurally isolated from each other as demanded by the isolation site theory for selective oxidation catalysis. Given that such idealized homogeneous distributions are unlikely, the V : Sb ratio of a selective catalyst probably will need to be less than 1/3 to achieve selective paraffin oxidation. The extent to which the magnesium enters the structure needs to be assessed. It is very likely, and supported by indications of the existence of a ternary phase [2], that the magnesium will contribute to the site isolation as is by analogy the case in $Al_{1-x}SbV_xO_4$ [13c]. Additional work is in progress to evaluate vanadium-lean Mg–V–Sb oxide catalysts in order to test this hypothesis.

4. Conclusions

A study of the oxidation kinetics of propane and propylene over $Mg_4V_2Sb_2O_x$ between 400 and 530°C, and 1 atm total pressure, reveals that propane is oxidized in parallel reactions to propylene, CO, and CO_2. The kinetics of oxidative dehydrogenation are zero-order in oxygen, whereas the deep oxidation kinetics are half-order in oxygen. All three reactions exhibit Langmuir-type dependence on the propane mole fraction, e.g.

$$r \propto \frac{kx}{1+Kx},$$

where x is the propane mole fraction and k and K are constants.

Propylene is also oxidized in parallel reactions to acrolein, CO, and CO_2. Like propane, partial oxidation of propylene is zero-order in oxygen, and the deep oxidation reactions are half-order in oxygen. The kinetics of all three reactions have Langmuir-type dependence on the propylene mole fraction.

The difference in the oxygen concentration dependence of the reaction kinetics indicates that distinct forms of reactive oxygen are involved in partial and deep oxidation of the hydrocarbons. Zero-order kinetics are indicative of reaction with lattice oxygen in the catalyst, and half-order kinetics are consistent with reaction with dissociatively adsorbed oxygen. The common dependence on hydrocarbon oxidation implies that a single form of adsorbed hydrocarbon takes part in partial and deep oxidation reactions; the hydrocarbon apparently adsorbs non-competitively with oxygen. A kinetic model based on these observations fits the kinetic data quantitatively.

Drawing on the oxidation catalysis literature, we have developed a working model of the mechanism (including active sites) by which propane is oxidized selectively and nonselectively over $Mg_4V_2Sb_2O_x$. This analysis indicates that vanadium ions, in the form of V–O· inorganic radicals, are necessary for activation of propane. If these centers are structurally isolated from each other in an antimony matrix, they are selective for partial oxidation to propylene. If, however, additional vanadium ions are adjacent to the active site, the additional electrophilic oxygen associated with these ions attacks the adsorbed hydrocarbon and produces CO_x. This analysis indicates that the selectivity of the catalyst can be improved by reducing its vanadium content, thereby reducing the number of sites with multiple vicinal vanadium ions. In addition, selective doping aimed at decreasing the amount and the electronegative character of the oxygen associated with the waste forming sites should reduce the waste forming reaction channel in favor of the selective oxydehydrogenation/oxidation channel.

Finally, it may be possible to minimize the amount of electrophilic chemisorbed oxygen and reduce CO_x production by operating in redox mode, i.e. in the absence of gas-phase oxygen. This strategy should work if exchange between adsorbed and lattice oxygen is slow on the time scale of the reactions.

An alternative approach might be to aim for a more stable useful, isolatable intermediate than propylene or acrolein. Such an intermediate of high commercial value is acrylonitrile. Therefore, it should be possible to convert propane in the presence of ammonia and oxygen (air) to acrylonitrile using a Mg–V–Sb-oxide catalyst of optimized composition; either alone or in the presence of a propylene to acrylonitrile catalyst such as the well known promoted Fe–Sb-based catalysts [9b,15].

Acknowledgement

The authors gratefully acknowledge D.J. Martenak, P.A. Agaskar, and J.G. Tsikoyiannis for their valuable contributions to this work.

Appendix. Derivation of rate equations

A.1. Partial oxidation

Partial oxidation of hydrocarbon (propane or propylene) occurs by reaction of adsorbed hydrocarbon with lattice oxygen. Assuming this reaction to be first-order in each reactant, the rate is:

$$r = k_{1\mathrm{s}} \theta_{\mathrm{C}_3} C_{\mathrm{O}_\mathrm{O}} , \tag{A1}$$

in which $k_{1\mathrm{s}}$ is the rate constant for partial oxidation on the surface, θ_{C_3} is the surface coverage of hydrocarbon and Co_O is the concentration of lattice oxygen at the catalyst surface. Hydrocarbon adsorption is assumed to be rapid and reversible, i.e. the hydrocarbon is in adsorption equilibrium, and the surface coverage is assumed to follow the Langmuir isotherm[#1]:

$$\theta_{\mathrm{C}_3} = \frac{K_{\mathrm{C}_3} P_\mathrm{T} x_{\mathrm{C}_3}}{1 + K_{\mathrm{C}_3} P_\mathrm{T} x_{\mathrm{C}_3}} , \tag{A2}$$

in which K_{C_3} is the adsorption equilibrium constant, P_T is the total pressure, and x_{C_3} is the hydrocarbon mole fraction. Reoxidation of the catalyst surface by gas-phase oxygen is assumed to be rapid compared to reduction by the hydrocarbon; therefore, the surface remains fully oxidized and $C_{\mathrm{O}_\mathrm{O}}$ is independent of gas-phase composition. Substituting for the hydrocarbon surface coverage and lattice oxygen concentration in the rate equation above yields:

$$r = \frac{k_{1\mathrm{s}} K_{\mathrm{C}_3} C_{\mathrm{O}_\mathrm{O}} P_\mathrm{T} x_{\mathrm{C}_3}}{1 + K_{\mathrm{C}_3} P_\mathrm{T} x_{\mathrm{C}_3}} . \tag{A3}$$

When the total pressure is 1 atm, eq. (A2) equals eq. (8), with $k_{\mathrm{Pr}} = k_{1\mathrm{s}} K_{\mathrm{C}_3} C_{\mathrm{O}_\mathrm{O}}$.

A.2. Deep oxidation

Deep oxidation of propane and propylene occurs by reaction of adsorbed hydrocarbon with dissociatively adsorbed oxygen. Assuming this reaction to be first-order in each reaction, the rate is:

$$r = k_{2\mathrm{s}} \theta_{\mathrm{C}_3} \theta_\mathrm{O} , \tag{A4}$$

where $k_{2\mathrm{s}}$ is the rate constant for deep oxidation on the surface and θ_O is the surface coverage of oxygen. The hydrocarbon is again assumed to be in adsorption equilibrium, and its coverage, θ_{C_3}, is described by eq. (A2). Oxygen is assumed to be in dissociative-adsorption equilibrium, and adsorption is non-competitive, i.e. oxygen and the hydrocarbon adsorb on different types of surface sites. The surface coverage is assumed to follow the Langmuir isotherm[#2]:

$$\theta_\mathrm{O} = \frac{(K_{\mathrm{O}_2} P_\mathrm{T} x_{\mathrm{O}_2})^{1/2}}{1 + (K_{\mathrm{O}_2} P_\mathrm{T} x_{\mathrm{O}_2})^{1/2}} , \tag{A5}$$

in which K_{O_2} is the oxygen adsorption equilibrium constant and x_{O_2} is the mole fraction of oxygen in the gas phase. Substitution for the surface coverages in eq. (A4) yields:

$$r = \frac{k_{2\mathrm{s}} K_{\mathrm{C}_3} P_\mathrm{T} x_{\mathrm{C}_3} (K_{\mathrm{O}_2} P_\mathrm{T} x_{\mathrm{O}_2})^{1/2}}{(1 + K_{\mathrm{C}_3} P_\mathrm{T} x_{\mathrm{C}_3})[1 + (K_{\mathrm{O}_2} P_\mathrm{T} x_{\mathrm{O}_2})^{1/2}]} . \tag{A6}$$

Assuming the surface coverage of oxygen to be small $(K_{\mathrm{O}_2} P_\mathrm{T} x_{\mathrm{O}_2})^{1/2} \ll 1$, eq. (A6) simplifies to:

$$r = \frac{k_{2\mathrm{s}} K_{\mathrm{C}_3} K_{\mathrm{O}_2} P_\mathrm{T}^{3/2} x_{\mathrm{C}_3} x_{\mathrm{O}_2}^{1/2}}{1 + K_{\mathrm{C}_3} P_\mathrm{T} x_{\mathrm{C}_3}} . \tag{A7}$$

At 1 atm total pressure, eq. (A7) equals eq. (10) with $k_{2\mathrm{s}} K_{\mathrm{C}_3} K_{\mathrm{O}_2}$.

References

[1] F. Cavani and F. Trifirò, Catal. Today 24 (1995) 307.
[2] J.N. Michaels, D.L. Stern and R.K. Grasselli, Catal. Lett. 42 (1996) 135.
[3] D.L. Stern, J.N. Michaels, L. DeCaul and R.K. Grasselli, Appl. Catal., in press.
[4] M.A. Chaar, D. Patel, M.C. Kung and H.H. Kung, J. Catal. 85 (1987) 483;
M.A. Chaar, D. Patel and H.H. Kung, J. Catal. 109 (1988) 463.
[5] D.S.H. Sam, V. Steinen and J.C. Volta, J. Catal. 123 (1990) 417.
[6] R.J.H. Voorhoeve, J.P. Remeika and L.E. Trimble, Ann. NY Acad. Sci. 272 (1976) 3.
[7] R.K. Grasselli and J.D. Burrington, Adv. Catal. 30 (1981) 131.
[8] C.G. Hill, *An Introduction to Chemical Engineering Kinetics and Reactor Design* (Wiley, New York, 1977) pp. 173–192.

[#1] If adsorbed hydrocarbon is in equilibrium with gas-phase hydrocarbon, $K_{\mathrm{C}_3} = a_{\mathrm{C}_3}^{(\mathrm{s})} / a_{\mathrm{C}_3}^{(\mathrm{g})}$, where $a_{\mathrm{C}_3}^{(\mathrm{s})}$ and $a_{\mathrm{C}_3}^{(\mathrm{g})}$ are the activities of the hydrocarbon on the surface and in the gas phase, respectively, and K_{C_3} is the adsorption equilibrium constant ($K_{\mathrm{C}_3} = \exp(\Delta G_{\mathrm{ads}}/RT)$, ΔG_{ads} = free energy of adsorption). Using a standard state of unit fugacity (ideal gas at 1 atm) and assuming gas-phase ideality, the gas-phase activity equals the partial pressure of the hydrocarbon. If hydrocarbon adsorption is ideal (fixed number of sites, no interactions between adsorbate molecules), the surface activity is related to surface coverage by: $a_{\mathrm{C}_3}^{(\mathrm{s})} = \theta_{\mathrm{C}_3} / (1 - \theta_{\mathrm{C}_3})$. Substitution for the activities and rearrangement yields eq. (A2), the Langmuir isotherm for non-dissociative adsorption.

[#2] If oxygen adsorbed competitively with the hydrocarbon, the oxygen surface coverage would be described by: $\theta_\mathrm{O} = (K_{\mathrm{O}_2} P_\mathrm{T} x_{\mathrm{O}_2})^{1/2} / [1 + K_{\mathrm{C}_3} P_\mathrm{T} x_{\mathrm{C}_3} + (K_{\mathrm{O}_2} P_\mathrm{T} x_{\mathrm{O}_2})^{1/2}]$ and the hydrocarbon surface coverage would be described by: $\theta_{\mathrm{C}_3} = K_{\mathrm{C}_3} P_\mathrm{T} x_{\mathrm{C}_3} / [1 + K_{\mathrm{C}_3} P_\mathrm{T} x_{\mathrm{C}_3} + (K_{\mathrm{O}_2} P_\mathrm{T} x_{\mathrm{O}_2})^{1/2}]$.

[9] (a) R.K. Grasselli, in: *Surf. Prop. and Catal. by Non-Metals*, eds. J. Bonelle et al. (Reidel, Dordrecht, 1983) p. 273;
(b) R.K. Grasselli, G. Centi and F. Trifirò, Appl. Catal. 57 (1990) 149;
(c) N.D. Spencer, C.J. Periera and R.K. Grasselli, J. Catal. 126 (1990) 546;
(d) G. Centi, E. Patane, F. Trifirò and R.K. Grasselli, Stud. Surf. Sci. Catal. 55 (1990) 515.

[10] J.D. Burrington, C.T. Kartisek and R.K. Grasselli, J. Catal. 87 (1984) 363.

[11] J. Haber, *Solid State Chemistry in Catalysis*, ACS Symp. Ser. 279 (Am. Chem. Soc., Washington, 1985) p. 3.

[12] V.D. Sokolovskii, React. Kinet. Catal. Lett. 37 (1988) 121.

[13] (a) J.L. Callahan and R.K. Grasselli, AIChE J. 9 (1963) 755;
(b) R.K. Grasselli and D.D. Suresh, J. Catal. 25 (1972) 273;
(c) J. Nilsson, A.R. Lana-Canovas, S. Hansen and A. Andersson, J. Catal. 160 (1996) 224.

[14] T. Birchall and A.W. Sleight, Inorg. Chem. 15 (1976) 868;
F.J. Berry, M.E. Brett and W.R. Patterson, J. Chem. Soc. Dalton Trans. (1983) 9;
A. Landa-Canovas, J. Nilsson, S. Hansen, K. Stahl and A. Andersson, J. Solid State Chem. 116 (1995) 369.

[15] Y. Sasaki, T. Nakamura, Y. Nakamura, K. Moriya, H. Utsumi and S. Saito, US Patent 4,370,279 (1983);
R.G. Teller, J.F. Brazdil and R.K. Grasselli, J. Chem. Soc. Faraday Trans. 81 (1985) 1693;
R.K. Grasselli, *Ammoxidation, Handbook of Heterogeneous Catalysis* B, 4.6.7., eds. G. Ertl, H. Knözinger and J. Weitkamp, in press.